FROM SPARKS TO PRECISION: PARAMETRIC OPTIMIZATION OF WIRE EDM FOR EFFICIENCY AND ACCURACY IN AL 6113 ALLOY MACHINING

Tijo D.[1,*], Liju Mathew Alexander[1], Job Thomas[1,2], Johnson Uthuppan[1,3], Sheik Shahban Shafeer[1], Parthip Manoj[1], and Vishnu K.V.[1]

Received: September 05, 2025; Revised: October 29, 2025; Accepted: November 11, 2025

Abstract

Wire-Electro Discharge Machining (WEDM) is a promising non-traditional machining process for aluminium alloys, which are otherwise difficult to machine using conventional methods due to plastic deformation and the formation of heat-affected zones. In the present study, the machinability of Al 6113 alloy was investigated under varying WEDM parameters using a Taguchi L9 orthogonal design. The influence of pulse-on time, pulse-off time, and peak current on material removal rate (MRR), kerf width, and surface morphology was systematically evaluated. The results indicate that pulse-on time is the most significant factor influencing both MRR and kerf width, while pulse-off time also plays a critical role in determining machining efficiency. Surface morphology analysis revealed that higher discharge energy conditions led to the formation of microcraters, micropores, and recast layers, whereas optimized parameters improved surface integrity. In addition, a Pareto front-based multi-objective optimization was employed to balance MRR and kerf width, identifying non-dominated solutions and a knee point for improved trade-offs between productivity and machining accuracy. The findings highlight the effectiveness of WEDM in machining Al 6113 alloy and establish its potential for precision applications in aerospace and automotive industries.

Keywords: **Al 6113 alloy; Kerf width; Material removal; Microstructure; Peak Current; Pulse on time; Wire-EDM**

---

[1] *Department of Mechanical Engineering, Saintgits College of Engineering (Autonomous), Kottayam, Kerala, India. E-mail: tijo.d@saintgits.org*; LIJU.MATHEW@saintgits.org; shahban.sheik@gmail.com; parthipmanoj.7@gmail.com; vishnukvcr091@gmail.com*

[2] *Department of Mechanical Engineering, Middlesbrough College, Middlesbrough, United Kingdom. E-mail: thomasjob2418@gmail.com*

[3] *Hochschule Wismar, University of Applied Sciences: Technology, Business and Design, Wismar, Germany. E-mail: johnsonuthuppan62@gmail.com*

[*] *Corresponding author*

DOI: https://doi.org/10.55766/sujst11362

Introduction

Over the years, industries such as aerospace, automobile and marine, aluminium and its alloys are extensively used due to its high specific weight and good corrosion properties (Pramanik *et al*., 2019; Srinivasan *et al*., 2024). Machining of Al alloy by conventional machining process results in adverse plastic deformation in the workpiece and further leads to the formation of significant heat affected zone (Riveiro *et al*., 2017; Sun *et al*., 2024). This highlights the importance of non-contact machining process to machine lightweight materials like Al and Mg alloys. Therefore, machining of light weight alloys by non-traditional machining process and further their optimisation of process conditions can be an advantage for these industries which reduces the overall cost, machining time and improves machining integrity. In WEDM, machining is performed using a wire electrode with no contact with the workpiece material. (Gao *et al*., 2025; Eaysin *et al*., 2025). In the last few decades or so Wire EDM is extensively employed for the machining of materials for commercial and industrial applications (Praveen *et al*., 2024). From the literatures, it is found that the non-contact machining can develop good surface finish and further the controllable spark can result in excellent machining integrity (Prakash *et al*., 2013; Van Riel *et al*., 2024). In WEDM process, the tool (wire) is continuously fed into the workpiece material and the potential difference between the electrodes results in sparking between them and material removal occurs by erosion. In WEDM, the spark between electrodes can be controlled by adjusting the different process conditions used in WEDM process (Paulson *et al*., 2023).

Over the years various researchers studied the significance of different machining conditions of Wire EDM on the MRR, kerf width on machining performance, along with surface morphology and topographical features. Mohapatra *et al*. (2014) examined the influence of WEDM conditions like pulse duration, pulse off time and wire feed rate while gear cutting from copper using WEDM process. From their study, it was found that Ton and Toff are the most significant parameters and optimum parameters were determined for maximum MRR and minimized pitch error. Anand *et al*. (2025) studied the impact of WEDM parameters on the characteristics of the surface of Al-Mg alloy and its composite. From their study it is revealed that the process parameters like pulse on time and applied current significantly enhances the roughness of the surface machined. Further, the kerf width and material removal also increased with increase in the above process parameters. But they reported that the enhancement in pulse off time reduces the removal of material, width of cut and surface quality. From this study it is revealed the quality of machined surface is highly depended on the process conditions employed while machining. Liao *et al*. (2004) reported that to achieve good surface finish the discharge energy is to be controlled. It is also found that positive polarity (workpiece as cathode) can result in enhanced surface finish. Rao *et al*. (2014) optimised WEDM process parameters for surface roughness, MRR and white layer for the machining of Al alloy (Aluminium2014 T6). They reported that sacrificing cutting efficiency is important to obtain quality surface finish and process parameters can significantly impact machining. Zhao *et al*. (2024) investigated the thermal effects and microstructural variations occurred in machining of thin-walled rare-earth gadolinium (Gd) components while cutting by wire-EDM and reported that the thermal impact can be reduced by controlling the process parameters. Chen *et al*. (2025) adopted a method called Ultrasonic elliptical vibration machining which improved the machinability of Al-Si alloys by reduced the cutting forces required also allowed periodic chip formation. It was found that by controlling the above process conditions the roughness of the machined surface is significantly reduced. This work highlights the importance of controlling process conditions while machining various types of alloys. Sunil *et al*. (2024) adopted advanced cooling techniques while machining of Inconel 625 by wire EDM and successfully reduced the surface roughness and controlled MRR and their study shows great promise for adopting optimization studies for Al alloy machining by wire EDM. Abdullah *et al*. (2024) used Grey Relational Analysis in order to find the apt process parameters and to study their effect on MRR and surface roughness on stainless-steel and they highlighted the importance of optimization to find the appropriate process conditions in machining. Unlike most existing studies, which focus on WEDM of steels and hard alloys, this work uniquely investigates the machinability of lightweight Al 6113 alloy using WEDM. The study establishes process–performance relationships specific to Al 6113, supported by regression modelling and microstructural validation, which has not been extensively reported in the literature. A comparative examination of mechanical and physical properties of Al 6113 alloy with commonly used aluminum alloys, Al 6061 and Al 6082, is depicted in Table 1 (Vinayaka *et al*., 2021; Hong *et al*., 2023; Elhadi *et al*., 2024) The table highlights differences in tensile strength, yield strength, elongation, hardness, corrosion resistance, and machinability, which may affect the response of materials during WEDM operations. In terms of machinability, Al 6113 is considered moderate due to its alloying ingredients, whereas Al 6061 and Al 6082 demonstrate better machining characteristics. These distinctions suggest that Al 6113 may display different machining responses under spark-thermal erosion in WEDM, thereby emphasizes that Al 6113 despite being less studied, is a promising candidate for machining investigations.

Table 1. Properties of Al 6113, Al 6061, and Al 6082 Alloys

Property	Al 6113	Al 6061	Al 6082
Tensile Strength	310 MPa	310 MPa	300 MPa
Yield Strength	276 MPa	276 MPa	260 MPa
Elongation	12-25%	12-25%	9%
Hardness (Brinell)	95 HB	95 HB	91 HB
Corrosion Resistance	Good	Good	Excellent
Machinability	Moderate	Good	Excellent

Materials and Methods

For the present work, commercially available aluminium plate (6113 alloy) is cut into 75 × 50 × 5 mm size and the surface is polished using different grades of emery paper to remove the surface impurities present and further cleaned with ethanol.

Machining process is performed using Excetek V400 CNC wire EDM machine. The dielectric medium used during wire cut is deionized water and electrode used is brass wire with 0.25mm diameter. In the present investigation, WEDM experiments were primarily controlled using pulse-on time (Ton), pulse-off time (Toff), and average current (Aon). However, other process parameters like wire feed rate, wire tension, open circuit voltage and dielectric flushing pressure kept constant during the experimentation. The controlled conditions ensured a reliable study on the effect of process parameters like Ton, Toff and Aon on the machining performance of Al 6113. The design for the present experiment is designated based on Taguchi method for the variation of Ton and Aon, the WEDM parameters with their levels used for initial stage is illustrated in Table 2, where Toff was kept constant at 12 µs, and the constant process conditions are summarized in Table 3. In the second stage to investigate the effect of pulse off time on machining performance, Toff was varied as shown in Table 4, while Ton and Aon were kept constant at 11 µs and 6 A, respectively, in addition to the constant process parameters listed in Table 3. These values were selected based on their stable performance range recognized in the first stage of experiments using the Taguchi approach. The schematic illustration of the WEDM process is shown in Figure 1.

Table 2. Variable wire EDM parameters and its levels

WEDM Parameters	Level 1	Level 2	Level 3
Pulse on time, Ton [µs]	10	11	12
Peak current, Aon [A]	5	6	7

Table 3. Fixed WEDM maching parameters

Wire feed rate [m/min]	10
Wire tension [N]	1.5
Open-circuit voltage [V]	50
Dielectric flushing pressure [MPa]	0.3

Table 4. Experimental conditions of pulse-off time

Toff [µs]	Ton [µs]	Aon [A]
10		
11	11	6
12		

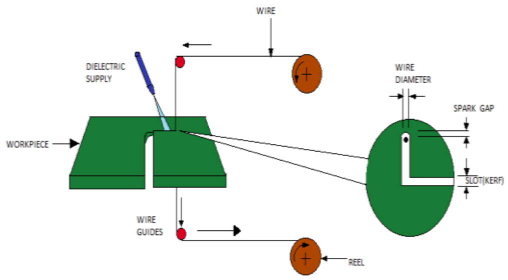

Figure 1. Wire EDM process schematic

Based on the Taguchi design nine experiments were performed initially and the influence of Ton and Aon on MRR, kerfwidth and microstructure is analysed. Additionally, the optimization of the WEDM process conditions is carried out using Taguchi L9 design by Minitab software. Further, the effect of pulse of time (Toff) is also studied by keeping Ton as 11 µs and Aon as 6 A. After the development of slots on Al alloy, the kerf width of the produced slot is measured using Tool makers microscope, and the amount of material removed is calculated using equation 1.

$$Material\ Removal\ Rate\ (MRR) = f \times Dw \times t \quad (1)$$

where; f feed rate;
Dw wire diameter;
t thickness of the AI 6113 alloy

Results and Discussions

Evaluation of Kerfwidth and Material removal rate

The variation of kerfwidth and MRR under different process conditions are depicted in Table 5. In the initial phase of the experiment, to examine the effect of pulse off time on Kerfwidth and MRR, other process parameters are kept constant during the WEDM cutting. The variation of Kerfwidth and MRR with increase in Toff is illustrated in Table 6. The constant parameters used are 6 A current and 11 µs pulse on time.

Further, to analyse the variation of WEDM parameters on MRR and Kerfwidth graphs were plotted. Figure 2 illustrates the impact of pulse on time and peak current on material removal. From Figure 2, it can observe that Ton has a significant impact on removal of material, however, there is no major change with the increase in Aon.

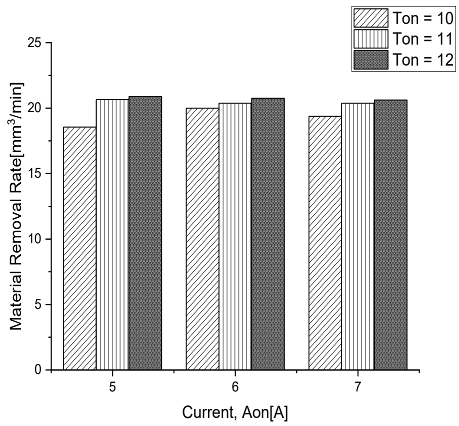

Figure 2. Variation of MRR with change in Ton and Aon

It is expected that with increase in Ton, the time to which the spark is in contact with Al 6113 alloy enhances and which further enhances the removal of material. In addition to that with increase in Ton the amount of energy available for cutting increases which again enhances the rate of removal of material (Balaji & Narendranath, 2023). For the present study, the influence of pulse-on-time (Ton) on material removal rate can be interrelated with the specific properties of Al6113 alloys as well. The increase in Ton enhances the duration of pulse and thereby increases the energy of the spark and which facilitates the higher material removal. The response of Al 6113 to this increased energy input is governed by its intrinsic characteristics, such as moderate thermal conductivity (lower than Al 6061 but higher than Al 7075) and relatively high mechanical strength. The moderate thermal conductivity of Al 6113 alloys mandates more sustained energy input for effective erosion of materials. Together, these factors elucidate that the enhancement in material removal rate with Ton observed in the present investigation, highlighting how the specific characteristics of an alloy impact the performance of WEDM.

From the data available in the current set of experiments it is revealed that Ton has more influence in material removal rate as compared to current (Aon). The variation of kerfwidth with increase in Ton and Aon is illustrated in Figure 3. The width of the slot (cut dimension) obtained during WEDM process is termed as kerf width. From the graph it is examined that kerf width increases with enhancement in peak current as current increases the intensity of spark increases, which result in the enhanced removal of material and which further increases the kerf width. It is also found that the kerf width changes positively with the

Table 5. MRR and Kerf width with variation of Aon and Ton

Exp.no	Aon [A]	Ton [µs]	MRR [mm^3/min]	Kerf width [mm]
1	5	10	18.5625	0.31
2	5	11	20.65	0.33
3	5	12	20.875	0.41
4	6	10	20	0.33
5	6	11	20.375	0.35
6	6	12	20.75	0.39
7	7	10	19.375	0.37
8	7	11	20.375	0.38
9	7	12	20.625	0.42

Table 6. Variation of MRR and Kerf width for different Toff conditions

Exp. no	Toff [µs]	Kerf width [mm]	MRR [mm^3/min]
1	10	0.36	21.2875
2	11	0.37	21
3	12	0.38	19.375

enhance in Ton value from 10 to 12 μs owing to the increase in energy of spark as it is in contact with workpiece for a longer duration. Additionally, with increase in the size of the crater develops for each pulse increases and thereby the kerf width also increases.

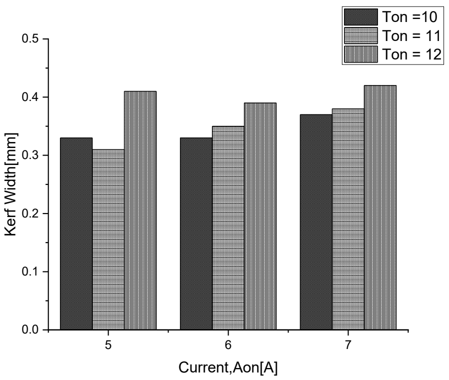

Figure 3. Variation in Kerfwidth with change in Ton and Aon

The variation kerf width and MRR with increase in Toff is depicted in Figure 4 and 5 respectively. From Figure 4, it is found that the material removal rate decreases with increase in pulse off time. The decrease in MRR with increase in pulse off time is due to the diminished size of crater due to lower energy input and reduced spark time during the cycle.

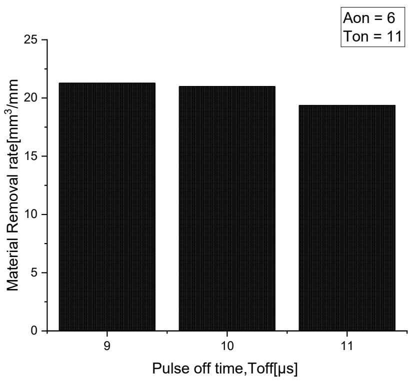

Figure 4. Impact of pulse off time on MRR

From Figure 5 it is observed that the increase in Toff results in a slight increase in kerf width. The increase is due to the better dielectric recovery owing to the longer pulse off time, leading to the more effect discharge of sparks in the succeeding pulses. The subsequent pulses produce larger localized molten pools, which laterally spreads before re-solidification and by this means widening the kerf. Furthermore, SEM microstructural observations of the machined surface have been included in the later part to validate the explanation.

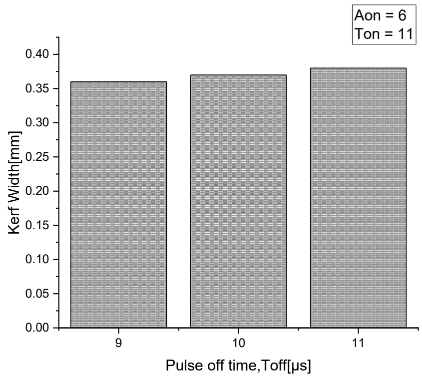

Figure 5. Impact of pulse off time on kerf width

Optimization of Process Parameters

The optimization of process parameters on MRR and kerf width is carried out using Minitab software by plotting graphs of means, Signal to noise (S/N) ratio and using the response table. The main effects plot for signal-to-noise (S/N) ratios considering Ton and Aon is depicted in Figure 6. In this analysis of MRR "Larger is Better" is considered and the response table reveals the rank of process paramters. Larger is better is considered due to more material removal is to be take place at optimum parameters, which is beneficial for the machining process. From the figure, it is found that Ton is a significant process parameter where with increase in Ton from 10 to 12 μs there is a substantial increase for S/N ratio. At lower Ton of 10 μs because of the lower energy input the MRR is significantly low. However, the effect of Aon on MRR is less significant. The S/N ratio increases from 5 to 6A and then reduces marginally when current further increased to 7A. This further shows that 6A current is the most favourable condition for achieving high MRR for this set of current values.

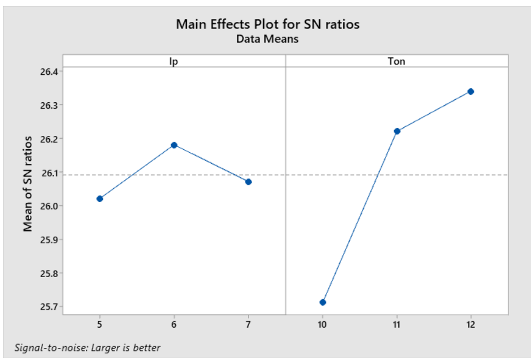

Figure 6. S/N ratio of MRR

From the response table depicted in Table 7 it is found that Ton has the highest delta value and is ranked one, which again shows Ton is the most significant parameter in the present investigation in comparison with peak current.

Table 7. Response for signal to noise ratio of MRR

Level	Ip	Ton
1	26.02	25.71
2	26.18	26.22
3	26.07	26.34
Delta	0.16	0.63
Rank	2	1

The Figure 7. illustrates the main effects plot for means of MRR, which shows how MRR varies with changes in pulse-on time and peak current, from the figure and response of means in Table 8 it is clear that the Ton is has a strong influence in material removal rate. This figure provides understanding into the average performance of peak current and Ton on MRR neglecting noise. Similar trend to S/N ratio can also observed in the main effect plot for mean values while S/N ratio graph is apt to identify the optimal WEDM parameters with noise while the means plot provide insight into overall efficiency.

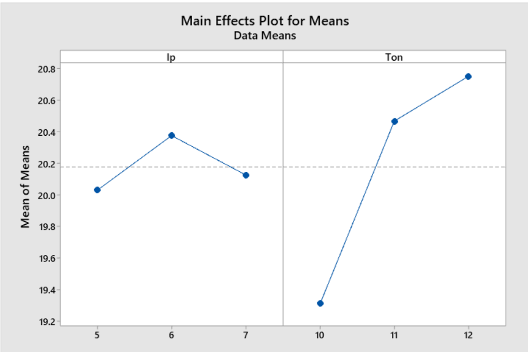

Figure 7. Mean of Material Removal Rate

Table 8. Response for means of MRR

Level	Ip	Ton
1	20.03	19.31
2	20.38	20.47
3	20.13	20.75
Delta	0.35	1.44
Rank	2	1

In case of Kerfwidth "Smaller is Better" is considered, because kerfwidth shows the accuracy of machining, a smaller kerf width represents improved control over the machining. Smaller is better criteria implies to minimize the output response like tool wear, surface roughness etc. From the graph illustrated in Figure 8 it is found that S/N ration reduces significantly with increase in Ton and which suggests lower Ton is favourable for minimizing the kerf width. Aon also provides a decreasing effect when current is increased from 5 to 7A. This result suggests that lower current and pulse on time contribute to better kerf width when the objective is to minimize kerf width. From the response data illustrated in Table 9 it is found that the Ton is significant parameter for controlling the kerf width.

Figure 8. S/N ratio for Kerfwidth

Table 9. Response for signal to noise ratio of kerf width

Level	Ip	Ton
1	9.182	9.479
2	8.976	9.051
3	8.192	7.819
Delta	0.991	1.660
Rank	2	1

The impact of WEDM process conditions on the kerf width was investigated using main effects plot for kerf width and response table for means of kerf width. From Figure 9 and Table 10 it is found that both Aon and Ton have significant influence on the kerf width while machining Al 6113 alloy by WEDM. The kerf width increases from 0.3500 to 0.3900 mm when Aon increased from 5 to 7A and this is because of the higher discharge energy more amount of material is removed laterally and this further widens the kerf developed. However, more significant influence can be observed on kerf width i.e. from 0.3367 to 0.4067 mm with increase in Ton to 12 µs. At high Ton owing to the longer duration of pulse more discharge energy is developed and this further deepens and widens the crater and which enhanced the width of kerf (Ali *et al.*, 2025). The response table further supports the mean effect plot quantitatively and delta value of 0.0700 for pulse on time as compared to 0.0400 for peak current depicts that pulse on time has significant impact on kerf width as compared to peak current and it is ranked as one. Overall, these finds suggests that lower discharge energy and smaller pulse durations are suitable for controlled removal of material from Al 6113 alloys.

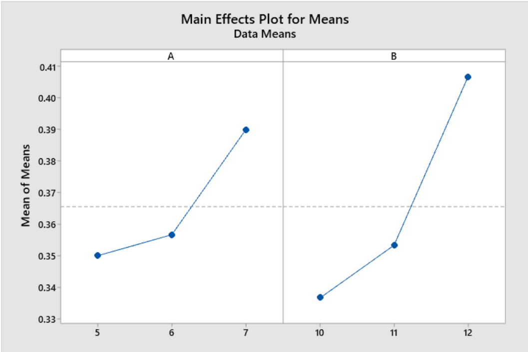

Figure 9. Mean of Kerfwidth

Table 10. Response for means of Kerf width

Level	Ip	Ton
1	0.3500	0.3367
2	0.3567	0.3533
3	0.3900	0.4067
Delta	0.0400	0.0700
Rank	2	1

Surface Morphology

SEM image of machined surface is analyzed on different magnifications. The SEM image produced at 7A (a) 10 µs (b) 12 µs for different 250 X and 500 X magnifications were illustrated in Figure 10. There is no significant variation is found from the SEM image of surface (a). In surface (b) there found micro pores on the magnified image, High discharge energy due to high Ton is the reason for craters or pores formed on the machined surface.

The morphology of the machined surface was examined using SEM images and the images at 250 and 500 X magnifications at peak current of 7 A with 10 µs and 12 µs pulse on time is illustrated in Figure 10. From the images it is revealed that there is significant changes in the surface morphology with the increase in pulse on time. When pulse on time is 10 µs the machined surface is more uniform and is almost defect free. At lower pulse on time owing to the short duration of pulse the molten material resolidified more uniformly and which results in fewer micro-voids and micro-pores. However, when Ton is increased 12 µs. However, when Ton is increased to 12 µs the surface shows more significant thermal defects with the presence of micropores as marked Figure 10. Further, this shows that material is removed as bulk for longer duration of pulse and which results in pronounced melting and poor removal of microchips. Additionally, the entrapped gas in the molten tool owing to long duration may result in the formation of micropores. These results further supporting the observations made on the influence of pulse on time on kerf width and MRR where longer duration of pulse resulted in enhanced material removal and surface disturbance. The presence of microcraters and micropores observed at higher discharge energy in the present work is consistent with the findings of Mandal *et al*. (2020), who also reported that at higher peak current and pulse on time enhances localized melting and rapid solidification on Al alloys during WEDM. The presence of micro pores at the machined surface, shows shorter pulse durations are preferable for applications where surface finish is important but at the expense of lower material removal.

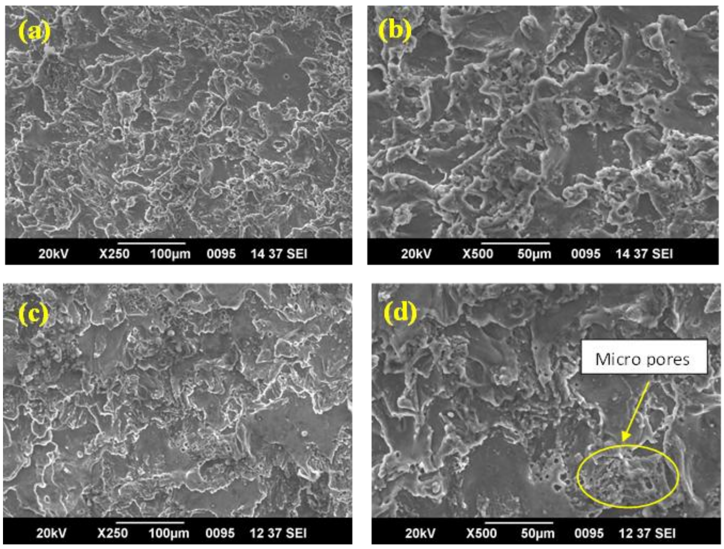

Figure 10. SEM image of machined surface produced at (a &b) 7 A, 10 µs for 250 X and 500 X magnifications, (c &d) 7 A, 12 µs for 250 X and 500 X magnifications

Figure 11 depicts the SEM images of the WEDM machined samples produced under 12 µs by varying current values: 5 A and 7 A. The surface was investigated at 250 and 500 X magnifications to study the morphological characteristics with the increase in current. The surface morphological characteristics like micro pores, recast layers, cracks etc. significantly impact the quality of surface produced. From the morphology of the machined surface produced at 5 A (top row) it is observed that several craters were formed due spark erosion machining. But the craters are not deep owing relatively low discharge energy and low thermal damage at 5 A current. There were some white layers present though which shows the debris are not flushed properly and some amount of material is resolidified and formed as a new layer on the surface machined. The morphology of Al alloy surface machined at 7A current is represented in the bottom row and from the figure it is clear that the number of irregularities is higher. Again, there are more pronounced craters on the surface at 7A suggest extreme melting and enhanced material removal at higher current values. Further, prominent recast layers were present at 7 A current indicating the re-deposition of microchips produced during machining. The above-mentioned features are further resulted in the development of micro pores on the Al alloy surface machined. Overall, the present study reveals that optimization of process conditions is extremely important to enhance productivity and surface integrity.

Figure 12 depicts the SEM images of the machined surface produced under higher Toff of 12 µs under constant pulse on time of 11 µs and peak current of 5 A. SEM images displays the presence of a white/recast layer along with localized micropores. The mentioned features are the characteristics of wire-EDM, where rapid heating and cooling results in micropores, cracks and deposition of resolidified material. The presence of recast layer and micropores further supports the discussion included for Figure 5, the longer Toff enhances the stability of spark and results in larger molten pool spreading and thereby widening the kerf.

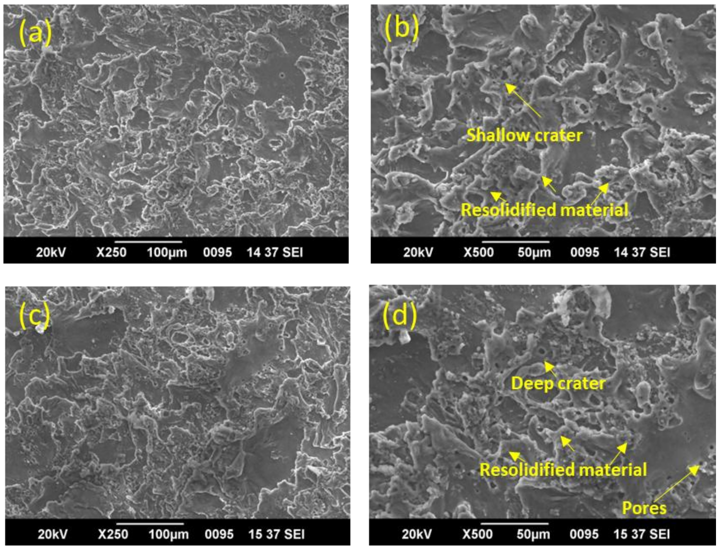

Figure 11. **SEM image of machined surface produced at (a &b) 12 µs, 5 A for 250 X and 500 X magnification, (c &d) 12 µs, 7 A for 250 X and 500 X magnification**

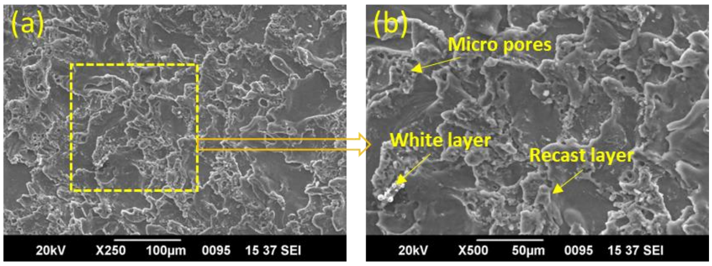

Figure 12. **SEM image of machined surface produced at pulse off time of 12 µs, with pulse on time of 11 µs and peak current of 5 A**

Regression Equation

Based on the present study a mathematical model (regression equation) is developed to predict the relationship between the output responses and input process paramters. The regression equation for MRR and kerf width is shown in Eqn.2 and Eqn.3 indicates Ton and Aon positively contribute to MRR and kerf width. In general, the relationship between paramters and ouput responses along with surface morphology provide a clear evidence on how process parameters influence the quality of surface machined. The regression model was statistically evaluated; the coefficient of determination (R^2) was computed to evaluate the reliability of model. The results exhibited higher R^2 values for MRR and kerfwidth for the present set of experiments, suggest good predictive accuracy of the regression equations.

$$MRR(mm^3/min) = -11.983 + 0.04792 \cdot A_{on} + 0.71875 \cdot T_{on}\ (R^2 = 0.94) \quad (2)$$

$$Kerf\ width = -0.1394 + 0.02 \cdot A_{on} + 0.035 \cdot T_{on}\ (R^2 = 0.91) \quad (3)$$

Model Validation and Error Analysis

The material removal rate (MRR) and kerf width of the Al-alloy workpiece were predicted using the regression models (Eqn.2 and 3) developed. For the machining conditions A_{on}=8 A and T_{on}=13 µs, the experimentally observed values were compared with the predicted values from the models. The comparison of values along with percentage of error is depicted in Table 11. The percentage of error is calculated using Eqn.4

$$Error\ (\%) = \frac{|Observed - Predicted|}{Observed}\ x\ 100 \quad (4)$$

From the analysis it is found that the present regression models predict the machining output response with reasonable accuracy. The small changes in observed values attributed to the experimental reservations and variations during the WEDM process. Overall, the regression models provide a reliable tool for predicting MRR and kerf width under similar process parameters in WEDM machining.

Table 11. Comparison of observed and predicted values

Parameter	Observed Value	Predicted Value	Error (%)
MRR (mm^3/min)	22.2875	21.7101	2.59
Kerf (mm)	0.45	0.4756	5.69

Pareto-based Multi-objective Optimization of Process Parameters

In WEDM machining process, it is very difficult to maximize MRR (productivity) and minimize kerf width (quality) at the same time since the objectives are contradictory. Therefore, multi-objective optimization employed to identify the trade-offs between high MRR and low kerf width usually represented as a Pareto front. In the present experimentation, the Pareto front was generated using the nine experimental conditions used, considering the objectives as MRR to be maximized and kerf width to be minimized. The non-dominated solutions from the nine trails forming the Pareto set are illustrated in Table 12.

Figure 13 depicts graphically the Pareto front obtained from the nine experiments used for Al alloy machining under various levels Ton and Aon. From the set of non-dominated solutions, Experiment 3 (Aon = 5 A, Ton = 12 µs, MRR = 20.875 mm³/min, Kerf = 0.41 mm) was identified as the knee point, the most balanced solution. The knee point depicts as the principle of compromise in multi objective optimization, representing the balance between productivity and machined surface quality as moving away from it would require a disproportionate trade-off between MRR and kerf width.

Table 12. Pareto-optimal solutions for MRR and Kerf width

Exp. No.	Aon (A)	Ton (µs)	MRR (mm³/min)	Kerf width (mm)	Remarks
1	5	10	18.5625	0.31	Pareto point
2	5	11	20.6500	0.33	Pareto point
3	5	12	20.8750	0.41	Knee point
6	6	12	20.7500	0.39	Pareto point
9	7	12	20.6250	0.42	Pareto point

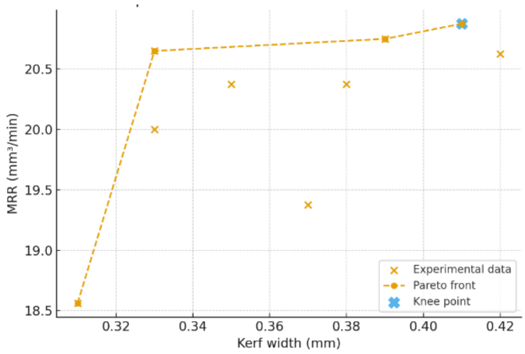

Figure 13. Experimental Pareto front of MRR vs Kerf width

Conclusions

In this work, Al 6113 alloy was effectively machined using the Wire Electro Discharge Machining (WEDM) technique, and the influence of process parameters on material removal rate (MRR), kerf width, and surface morphology was systematically investigated. The following conclusions can be drawn:

1. Peak current and pulse-on time contributed positively to both MRR and kerf width, with pulse-on time identified as the most significant factor. Increasing pulse-off time reduced material removal but simultaneously increased kerf width.

2. Surface morphology analysis using SEM confirmed that higher discharge energy, associated with increased peak current and pulse-on time, led to the formation of microcraters, micropores, and a recast layer on the machined surface.

3. A regression model was developed to establish a mathematical correlation between process parameters and performance measures, showing good agreement with experimental results and validating its suitability for prediction and optimization.

4. Multi-objective optimization using the Pareto front method highlighted the trade-off between maximizing material removal rate and minimizing kerf width. The identified non-dominated solutions, and particularly the knee point, provide balanced parameter settings for achieving high MRR and low kerf width.

Overall, the study highlights the importance of optimizing WEDM parameters to achieve improved machining performance and surface integrity in Al 6113 alloy, thereby demonstrating its potential for high-precision industrial applications.

Limitations and Future Scope

The present experiments have certain limitations, as it was restricted to Al 6113 alloy and the influence of most significant parameters like pulse on time, pulse off time and peak current is investigated. Future work can be directed towards studying the effect of parameters like wire tension, dielectric flushing pressure, and wire material by extending the research to other Al alloys and composites. Furthermore, the surface integrity evaluation can be directed toward extending detailed investigation of residual stresses, microhardness, corrosion resistance or fatigue behaviour.

Funding

The authors declare that there are no funds or grants received for performing this experimental work.

Authors' contributions

Tijo D: Conceptualization, Supervision and Writing original draft. Liju Mathew Alexander: Review and editing. Job Thomas, Johnson Uthuppan, Sheik Shahban Shafeer, Parthip Manoj and Vishnu KV: Methodology, Experimentation, Testing.

Declaration of AI technology usage

We declare that no Artificial Intelligence (AI) technologies or AI-assisted tools were utilized in any capacity during the writing and preparation of this article.

Conflicts of interest

The authors confirm that there is no conflict of interest related to the publication of the present work.

Acknowledgments

Authors thank Saintgits College of Engineering (Autonomous), Kottayam (India), Keltron Toolroom Research & Training Centre (KELTRAC), Kochi (India) and Sophisticated Test and Instrumentation Centre, CUSAT, Kochi (India) for the facilities provided to perform the experiments and characterisation.

References

Abdullah, M. A., Ahmed, B. A., & Ghazi, S. K. (2024). Enhancing material removal rate and surface roughness in wire EDM process using grey relational analysis. *Engineering, Technology & Applied Science Research, 14*(5), 17422–17427. https://doi.org/10.48084/etasr.8450

Ali, S., Ali, L., Imran, S. H., Khan, W. A., & Ali, H. (2025). Optimization of process parameters for precise corner accuracy in wire electric discharge machining of AISI D2 tool steel. *The International Journal of Advanced Manufacturing Technology*, 1–19. https://doi.org/10.1007/s00170-025-15998-7

Anand, G., Sardar, S., Sah, S., Guha, A., Albaijan, I., & Das, D. (2025). Surface and subsurface characteristics of wire-electrical discharge machined Al-alloy and composite: A fundamental study on the role of machining variables. *Journal of Materials Research and Technology, 36*, 9432–9461. https://doi.org/10.1016/j.jmrt.2025.05.126

Balaji, V., & Narendranath, S. (2023). Optimization of wire-EDM process parameters for Ni–Ti–Hf shape memory alloy through particle swarm optimization and CNN-based SEM-image classification. *Results in Engineering, 18*, Article 101141. https://doi.org/10.1016/j.rineng.2023.101141

Chen, D., Zheng, Z., Wu, D., Zeng, C., Zang, Y., She, Z., & Xu, J. (2025). Investigation on the machining mechanism and surface integrity in ultrasonic elliptical vibration cutting of Al-Si alloys. *Precision Engineering, 93*, 559–575. https://doi.org/10.1016/j.precisioneng.2025.02.007

Eaysin, A., Zinnah, M. A., Nayem, M., Begum, H. A., Protyai, M. I. H., Ashrafi, S., & Rashid, A. B. (2025). Prediction and optimization of surface quality and material removal rate in wire-EDM cutting of tungsten–copper alloy (W70Cu30). *Results in Surfaces and Interfaces, 18*, Article 100409. https://doi.org/10.1016/j.rsurfi.2024.100409

Elhadi, A., Zidaan, A., Abbas, H., Zaki, M., & Dakhil, M. (2024). Normal temperature mechanical properties of 6082 aluminium alloy as a function of tempering temperature: Experimental and numerical approach. *Acta Mechanica et Automatica, 18*(3), 385–392. https://doi.org/10.2478/ama-2024-0042

Gao, H., Gong, Y., Zhu, R., & Jin, L. (2025). Processing quality prediction and multi-objective optimization of polysilicon wire-EDM. *Materials Science in Semiconductor Processing, 192*, Article 109462. https://doi.org/10.1016/j.mssp.2025.109462

Hong, T., Ding, F., Chen, F., Zhang, H., Zeng, Q., & Wang, J. (2023). Mechanical properties of 6061 aluminum alloy under cyclic tensile loading. *Crystals, 13*(8), Article 1171. https://doi.org/10.3390/cryst13081171

Liao, Y. S., Huang, J. T., & Chen, Y. H. (2004). A study to achieve a fine surface finish in wire-EDM. *Journal of Materials Processing Technology, 149*(1–3), 165–171. https://doi.org/10.1016/j.jmatprotec.2003.10.034

Mandal, K., Bose, D., Mitra, S., & Sarkar, S. (2020). Experimental investigation of process parameters in WEDM of Al 7075 alloy. *Manufacturing Review, 7*, Article 30. https://doi.org/10.1051/mfreview/2020021

Mohapatra, K. D., & Sahoo, S. K. (2014). Parametric optimization of wire EDM process for gear cutting. *Journal of Basic and Applied Engineering Research, 1*(3), 78–84.

Paulson, D. M., Saif, M., & Zishan, M. (2023). Optimization of wire-EDM process of titanium alloy-Grade 5 using Taguchi's method and grey relational analysis. *Materials Today: Proceedings, 72*, 144–153. https://doi.org/10.1016/j.matpr.2022.06.376

Prakash, J. U., Moorthy, T. V., & Peter, J. M. (2013). Experimental investigations on machinability of aluminium alloy (A413)/fly ash/B4C hybrid composites using wire EDM. *Procedia Engineering, 64*, 1344–1353. https://doi.org/10.1016/j.proeng.2013.09.216

Pramanik, D., Kuar, A. S., & Bose, D. (2019). Effects of wire EDM machining variables on material removal rate and surface roughness of Al 6061 alloy. In *Renewable Energy and Its Innovative Technologies* (pp. 231–241). Springer. https://doi.org/10.1007/978-981-13-2775-9_20

Praveen, N., Kumar, N. S., Prasad, C. D., Giri, J., Albaijan, I., Mallik, U. S., & Sathish, T. (2024). Effect of pulse time (Ton), pause time (Toff), peak current (Ip) on MRR and surface roughness of Cu–Al–Mn ternary shape memory alloy using wire EDM. *Journal of Materials Research and Technology, 30*, 1843–1851. https://doi.org/10.1016/j.jmrt.2024.03.122

Rao, P. S., Ramji, K., & Satyanarayana, B. (2014). Experimental investigation and optimization of wire EDM parameters for surface roughness, MRR and white layer in machining of aluminium alloy. *Procedia Materials Science, 5*, 2197–2206. https://doi.org/10.1016/j.mspro.2014.07.426

Riveiro, A., Quintero, F., Del Val, J., Boutinguiza, M., Wallerstein, D., Comesaña, R., & Pou, J. (2017). Laser cutting of aluminum alloy Al-2024-T3. *Procedia Manufacturing, 13*, 396–401. https://doi.org/10.1016/j.promfg.2017.09.028

Srinivasan, D., Fakkir, M., Lenin, K., Pandiyan, G. K., & James, D. J. D. (2024). Evaluation of wire electrical discharge machining performance features on EN AW 6082 T6 aluminum alloy and optimization of machining characteristics. *Journal of Materials Engineering and Performance, 33*, 3546–3558. https://doi.org/10.1007/s11665-023-08234-4

Sun, Z., Geng, D., Guo, H., Ge, E., Zhou, E., Fan, Z., Meng, F., Jiang, X., & Zhang, D. (2024). Influence of transversal vibration on cutting performance and surface integrity during ultrasonic peening drilling of Al-Li alloys. *Chinese Journal of Aeronautics, 37*(10), 493–507. https://doi.org/10.1016/j.cja.2024.04.017

Sunil, B. D. Y., Goyal, A., Kumar, L., *et al*. (2024). Optimizing wire electrical discharge machining performance of Inconel 625 with genetic algorithms and particle swarm optimization. *Journal of Materials Research and Technology, 31*, 555–569. https://doi.org/10.1016/j.jmrt.2024.06.079

Van Riel, T., Qian, J., & Lauwers, B. (2024). Surface integrity of 316L steel machined sequentially by wire EDM and wire ECM. *Procedia CIRP, 123*, 256–261. https://doi.org/10.1016/j.procir.2024.05.046

Vinayaka, N., Lakshmikanthan, A., Patel, G. M., & Pon, C. (2021). Mechanical, microstructure and wear properties of Al 6113 fly ash reinforced composites: Comparison of as-cast and heat-treated conditions. *Advanced Materials Processing Technologies*, 1–16. https://doi.org/10.1080/2374068X.2021.1927649

Zhao, L., Shi, S., Li, Z., *et al*. (2024). Investigation of thermal deformation and surface microstructure of wire electrical discharge machining for thin-walled rare earth gadolinium. *Materials Today Communications, 39*, Article 108827. https://doi.org/10.1016/j.mtcomm.2024.108827